PROCEEDINGS OF ECOS 2026 - THE 39TH INTERNATIONAL CONFERENCE ON

EFFICIENCY, **C**OST, **O**PTIMIZATION, **S**IMULATION AND ENVIRONMENTAL IMPACT OF ENERGY SYSTEMS

28 JUNE – 03 JULY, 2026, CONSTANTA, ROMANIA

Optimal integration of latent heat thermal energy storage in EV thermal management systems: thermo-physical analysis of storage performance and waste heat utilisation

Ernest Zdanowicz[a]; Pouriya H. Niknam[b], Timothy Gordon[c], Chris Bingham[d], Simon Palmer[e]

[a] University of Lincoln, Lincoln, United Kingdom, 27202456@students.lincoln.ac.uk
[b] University of Lincoln, Lincoln, United Kingdom, phniknam@lincoln.ac.uk, CA
[c] University of Lincoln, Lincoln, United Kingdom, tgordon@lincoln.ac.uk
[d] University of Lincoln, Lincoln, United Kingdom, cbingham@lincoln.ac.uk
[e] WATT Electric Vehicle Company, Cornwall, United Kingdom, simon.palmer@wattelectricvehicles.com

Abstract

Electric Vehicles (EVs) face significant thermal management challenges, particularly during fast-charging and conditions where the battery temperature sits outside of the optimal range of 20-30℃ leading to accelerated degradation and reduced driving range. Whilst phase-change materials (PCMs) have been widely studied for improving temperature uniformity and distribution between battery cells, their potential as thermal energy storage (TES) devices within an EV thermal loop remains largely unexplored. This study investigates the viability of a passive latent heat thermal energy storage (LHTES) strategy for waste heat capture during fast-charging and the recycling of heat back into the battery pack and cabin heating system. A lumped thermal model of a 225-cell lithium-ion (nickel-manganese-cobalt (NMC)) battery module was developed in MATLAB Simulink, and Python Battery Mathematical Modelling (PyBaMM) library using the Bernardi heat generation equation and energy balance against experimental data for a standard charge case, with results consistently within a $\pm 2\%$ margin and a root mean square error of 0.35. A basic sensitivity analysis across PCM mass and thickness parameters from 2-50kg and 4-115mm demonstrated that a more compact PCM configuration results in a greater liquid volume fraction, indicating a better utilisation of the latent heat. The 2kg case achieved a peak battery temperature reduction of 21.7% when compared to the no-PCM, natural convection-only cooling case, storing approximately 84.3Wh of latent heat over a single fast-charge cycle. However, peak battery temperature across all cases remained above the upper optimal limit of 30℃, indicating that passive PCM cooling alone is insufficient and would require active cooling support. The stored energy of 84.3Wh was found to exceed the 22.2Wh requirement to raise battery module temperature from a cold-start condition of 0℃ into the optimal temperature range, leaving a margin of approximately 27% to account for thermal losses, establishing proof of concept for LHTES as a pre-conditioning energy source.

Keywords:

Battery thermal management; Electric vehicles; Latent heat storage; Phase-change materials; Waste heat recovery.

1 Introduction

Lithium-ion batteries have become a common find in modern Electric Vehicle (EV) design due to their high energy density and fast-charging capabilities [1], [2], which provides benefits over both Internal Combustion Engines (ICEs) and other battery chemistries, resulting in a significant rise for the EV market, with the IEA Global EV Outlook 2025 reporting global EV sales surpassing 17 million units sold in 2024. However, despite these benefits, their efficiency and performance in cold-start conditions results in significantly decreased range [3] as a result of suppressed electrochemical reaction rates due to being significantly outside of the optimal battery temperature range, which is typically placed between 20-30℃, as shown in Figure 1, from the review of thermal management of Lithium-ion batteries conducted by Hamid et. al. (2024). To mitigate this issue, there have been several types of thermal management systems developed in recent years, which are classified by Gharehghani et al. (2024) into Active, Passive, or Hybrid Cooling, and External or Internal Heating systems [4], all of which have made use of Phase-change materials (PCMs) in some capacity.

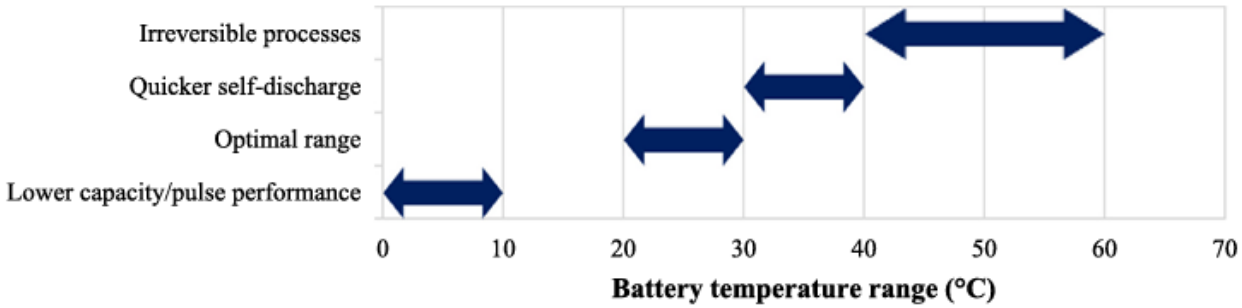

Figure 1. Effect of battery temperature range [5].

PCMs have easily found their way into EV battery development, with several studies implementing their use in-between battery cells to improve the cell temperature distribution by acting as a thermal buffer. This study aims to determine the viability of using a hybrid coolant and PCM thermal management strategy to store waste thermal energy, as well as the potential for more efficient heat routing towards the cabin and battery. Since the focus of this study does not rely on any chemical characteristics of the relevant components and is primarily concerned with the thermal characteristics, a simpler battery model can be afforded. Figure 2 shows the proposed system heat flow schematic, with a temperature sensor at the inlet and outlet of the battery pack to feed into a control loop which decides flow direction and priority between Battery pack for increased performance and the Cabin HVAC system for passenger comfort.

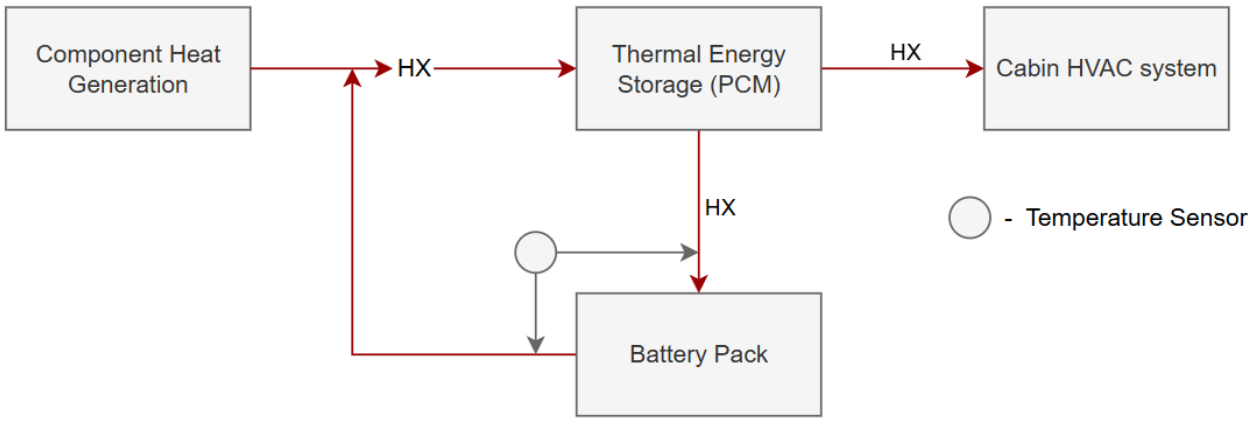

Figure 2. Thermal Storage System Schematic. (HX=Heat Exchanger).

Whilst the use of PCMs has become a popular research point in recent years, there are few papers which acknowledge its use for energy storage capabilities when it comes to the EV application, with most aiming for better temperature distribution between battery cells such as the work of Fang et al. [6], and whose works can still be used at a foundational level for battery modelling and heat characterisation. Looking at other notable uses of PCMs in thermal energy storage is also beneficial towards a greater understanding of their capabilities, such as looking at the PCM-Eff project, which focuses on latent heat storage and investigates PCM viability in Cooling storage for refrigeration equipment [7] through the design of a PCM-based heat accumulator.

The work of Mandev et al. [8] will serve as a fundamental design for the PCM heat battery, where Mandev focuses on the charge and discharge processes of the heat battery, whereas this research is concerned with quantifying waste heat potential and optimisation of thermal storage module topology for optimal heat storage

and discharge, which may use some elements of the topological optimisation of a PCM storage module heat exchanger through the work of Kim et al. [9].

With this study, the goal is to answer the question regarding their viability for storing energy within an EV coolant loop for open-case batteries, and whether the waste heat captured and recycled provides any technoeconomic benefits, such as increased range, as well as providing proof of concept for the future of PCM Thermal Storage development.

2 Novelty and contribution

As mentioned, the most common use for PCMs in EVs is to improve the temperature distribution between components, rather than to be captured and reused throughout the system. This research aims to:

a) Determine the system-level performance of LHTES for storing thermal energy to be reused and recycled to the battery or cabin on demand.
b) Develop a non-intrusive and non-disruptive thermal management system with seamless integration to a typical EV coolant loop.
c) Analyse the range impact on an EV travelling in a variety of conditions.
d) Lay a foundation which can be used to implement control logic for preconditioning algorithms to ensure stored heat is not allowed to dissipate and therefore be wasted.

3 Methodology

3.1 Theoretical background

To determine waste heat recovery potential, it is first necessary to find the battery heat generation, which was done by using the Bernardi battery heat equation (eqn. (1)) for the irreversible, joule heating term (I^2R) and reversible, entropic heat term $\left(I\,T\frac{\partial U}{\partial T}\right)$, where I is the current load at each time step, U is the open circuit voltage, R is the internal cell resistance as a function of the cell state of charge (SOC) and internal temperature, T. $\frac{\partial U}{\partial T}$ can also be referred to as the entropic coefficient.

$$Q_{battery}[W] = I(t)(U-V) + I(t)\left(T\frac{\partial U}{\partial T}\right) = \underbrace{I(t)^2R(SOC,T)}_{Q_{joule}} + \underbrace{I(t)\,T\frac{\partial U}{\partial T}}_{Q_{rev}} \quad (1)$$

EV fast charging is typically separated into constant current (CC), tapering, constant voltage (CV), and trickle charging [10]. The first stage, CC charging, is also referred to as the fast charging, where joule heating dominates due to the increased C-rate, meaning that the entropic heat generation can be discounted. For this study, the battery heat generation was considered between 20% to 80% SOC, to align with the optimal charge pattern for lithium-ion batteries. Battery parameter data for the LG Chem INR21700 M50 cell was used due to its availability as a standard dataset of the Python Battery Mathematical Modelling library (PyBaMM), which was used to generate a heat profile to be used as an input for a MATLAB Simulink model. The energy balance equation (eqn. (2)) was used to determine the cell temperature and was then compared to the experimental data collected from the Chen 2020 dataset [11].

$$mC_p\frac{dT}{dt} = I^2R(SoC,T) - hA(T-T_{cool}) \quad (2)$$

The battery itself is modelled as a heat generation source with a thermal mass, shown in Figure 3, with the heat generation profile (heat_ts) as the input to a thermal mass, with convection in parallel, as per standard thermal circuit assembly.

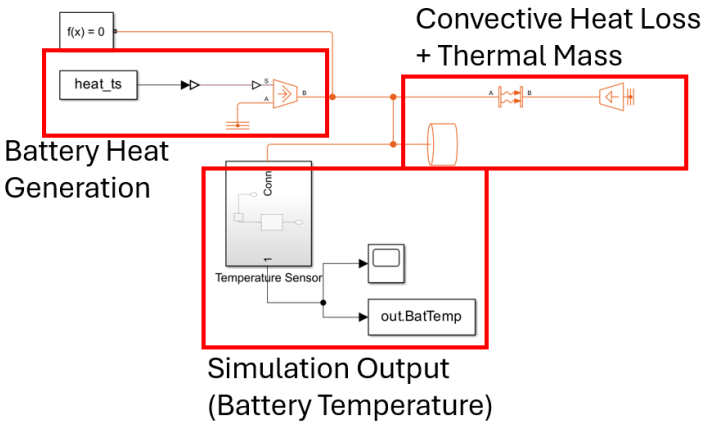

Figure 3. Simplified battery Simulink model.

Since this study is not explicitly focused on individual cell behaviour, a lumped thermal model was considered appropriate for pack and module level analysis, rather than cell-core analysis. Figure 4 illustrates the heat generation profile of a 15S15P (Total 225 Cell) module, with a peak of approximately 455W during the fast-charging cycle. A full fast-charging cycle takes approximately 4600s, or approximately 1 hour and 20 minutes, whereas a standard charge cycle takes approximately 14100s, or approximately 4 hours, dictating the simulation runtime for the temperature profiles.

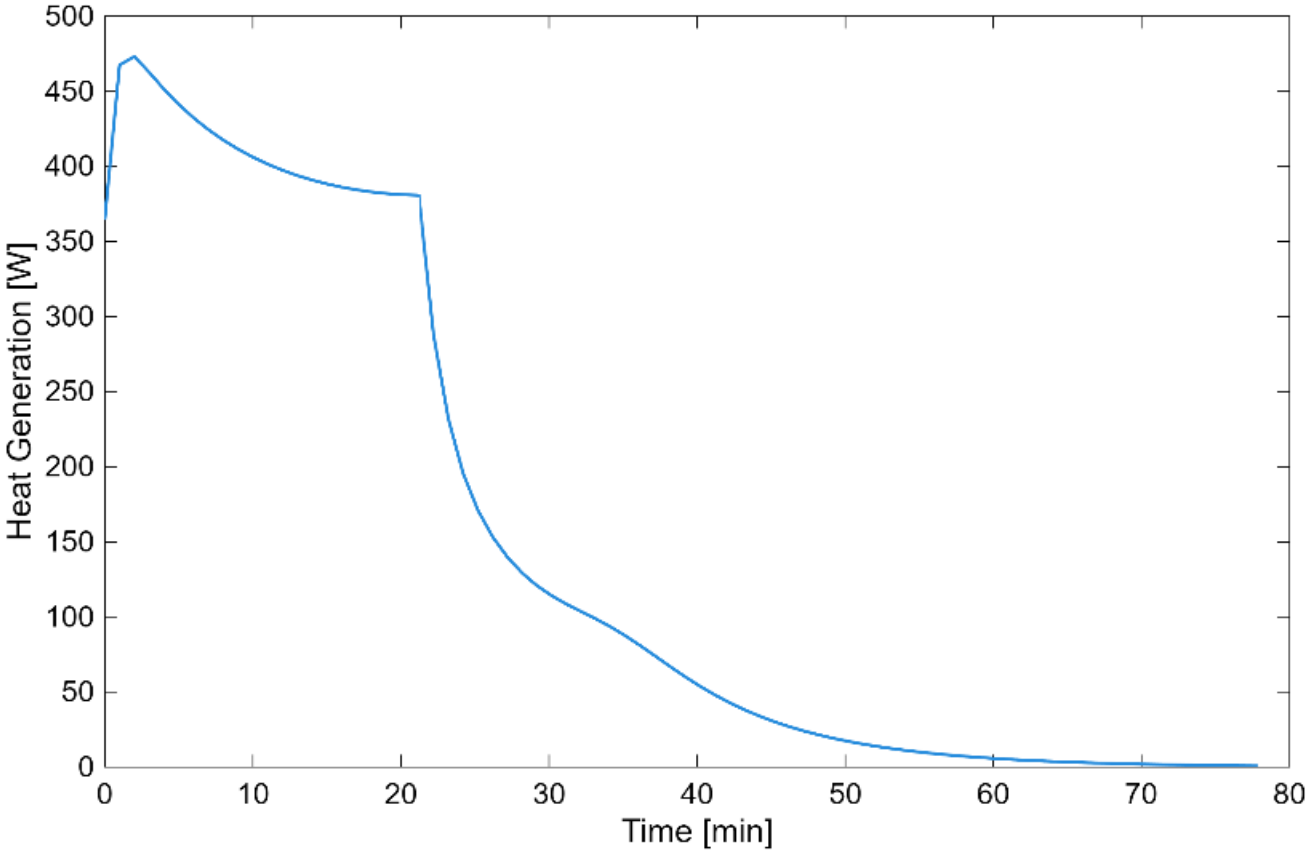

Figure 4. Battery total heat generation profile.

3.1.1 LHTES modelling

Alongside total waste heat generated by the battery, the maximum heat storage capacity, Q_{TES}, of the TES module was calculated using eqn. (3), where m_{pcm} is the mass of phase-change material, and L is the latent heat of fusion. The total heat storage capacity is then compared to the ratio of total heat input, Q_{in}, to determine the liquid volume fraction, ϕ_L, of the PCM at each time step (eqn. (4)).

$$Q_{TES}[kJ] = m_{pcm}L \tag{3}$$

$$\phi_L(t) = \frac{Q_{in}(t)}{Q_{TES}} \tag{4}$$

For this study, the PCM was modelled using energy balance to determine the phase state, where the model uses sensible heat until the melting temperature, T_m, is reached, at which point the PCM temperature, T_{pcm} is held until the PCM is fully melted, as described algebraically in eqn. (5) [12].

$$Q_{PCM}[kJ] = \begin{cases} mC_p(T_m - T_{pcm}) & T_{pcm} < T_m : \phi_L = 0 \\ mL & T_{pcm} = T_m : 0 < \phi_L \leq 1 \\ mC_p(T_m - T_{pcm} & T_{pcm} > T_m : \phi_L = 1 \end{cases} \tag{5}$$

Figure 5 shows the Simulink architecture used for the model.

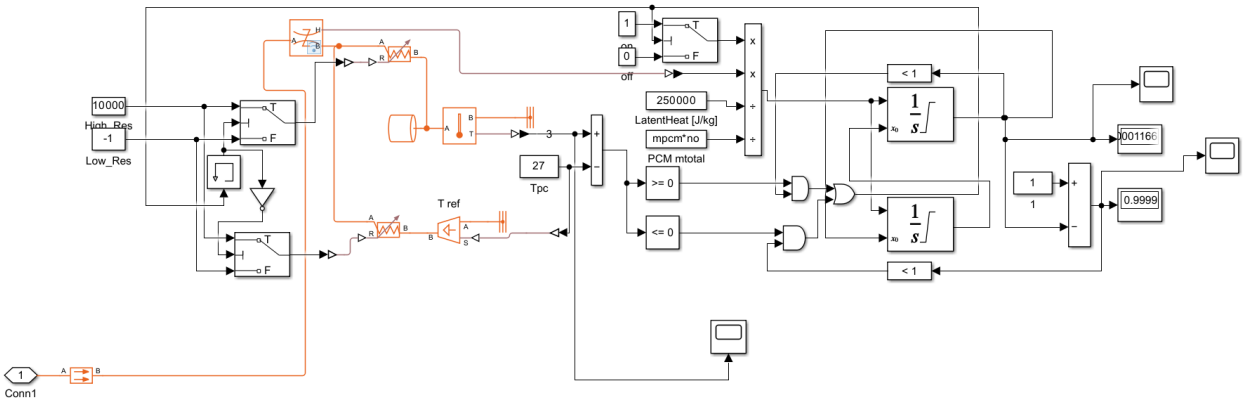

Figure 5. Simulink PCM architecture.

Figure 6 illustrates this system in a simplified schematic, which shows battery pack heat loss via convection to the atmosphere, and via conduction towards the PCM module.

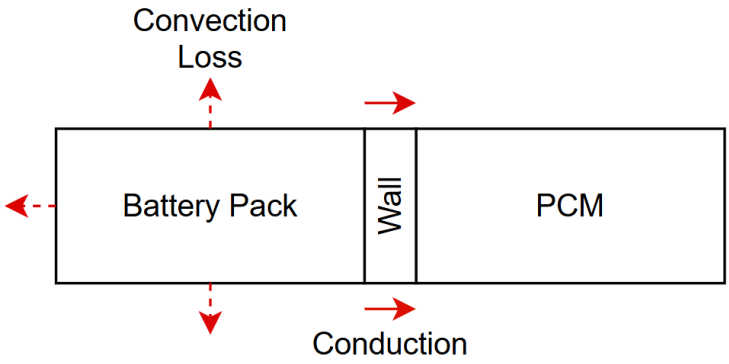

Figure 6. Simplified system diagram.

Table 1 shows the initial conditions considered for the lumped thermal model, Simulated using MATLAB for a 1-dimensional overview of battery heat generation. The parameters used for the PCM are consistent with a typical, paraffin-based PCM.

Table 1. Lumped Thermal Model Initial and Boundary Conditions.

Parameter	**Symbol**	**Value**	**Unit**
Cell Capacity	Q_n	5	Ah
Cell mass	m_{cell}	55	g
Ambient Temperature	T_{amb}	26	℃
No. Series Cells	N_s	15	-
No. Parallel Cells	N_p	15	-
Coefficient of Heat Transfer	h	5	$Wm^{-2}K^{-1}$
Specific Heat Capacity (Cell)	$C_{p(cell)}$	900	$Jkg^{-1}K^{-1}$
PCM Melting Temperature	T_m	28	℃
Specific Latent Heat (PCM)	L	160000	Jkg^{-1}
Specific Heat Capacity (PCM)	C_{pcm}	2300	$Jkg^{-1}K^{-1}$
PCM Mass	m_{pcm}	20	kg
Thermal Conductivity (PCM)	k_{pcm}	0.2	$Wm^{-1}K^{-1}$

4 Results and discussion

4.1 Case study validation – base case

Temperature data of the battery was validated with a standard-charge case; The higher C-rate, fast-charging cycle is treated as a model-based prediction, where the underlying simulation parameters and physics excluding the input current are held consistent to ensure that the model structure is validated. Results for the standard-charge fall consistently within a $\pm 2\%$ margin and a root mean square error (RMSE) of 0.35, which is deemed acceptable for the thermal lumped model used. As previously mentioned, the simulation runtime in this case was dictated by the length of a standard charge cycle, meaning that the fast charge curve peaks and

stabilises significantly earlier in comparison. This does, however, provide a reasonable check to ensure that the battery temperature returns to the ambient state once the charge is complete, as expected, shown in Figure 7. The model results are consistent with similar models found in literature regarding a 21700 NMC cylindrical cell lumped thermal model, with a peak of approximately 49.5℃ being consistent with a 1.5C charge, where peak temperature of 50-60℃ is reported at 2C, providing indirect confidence towards the model's predictive accuracy [13].

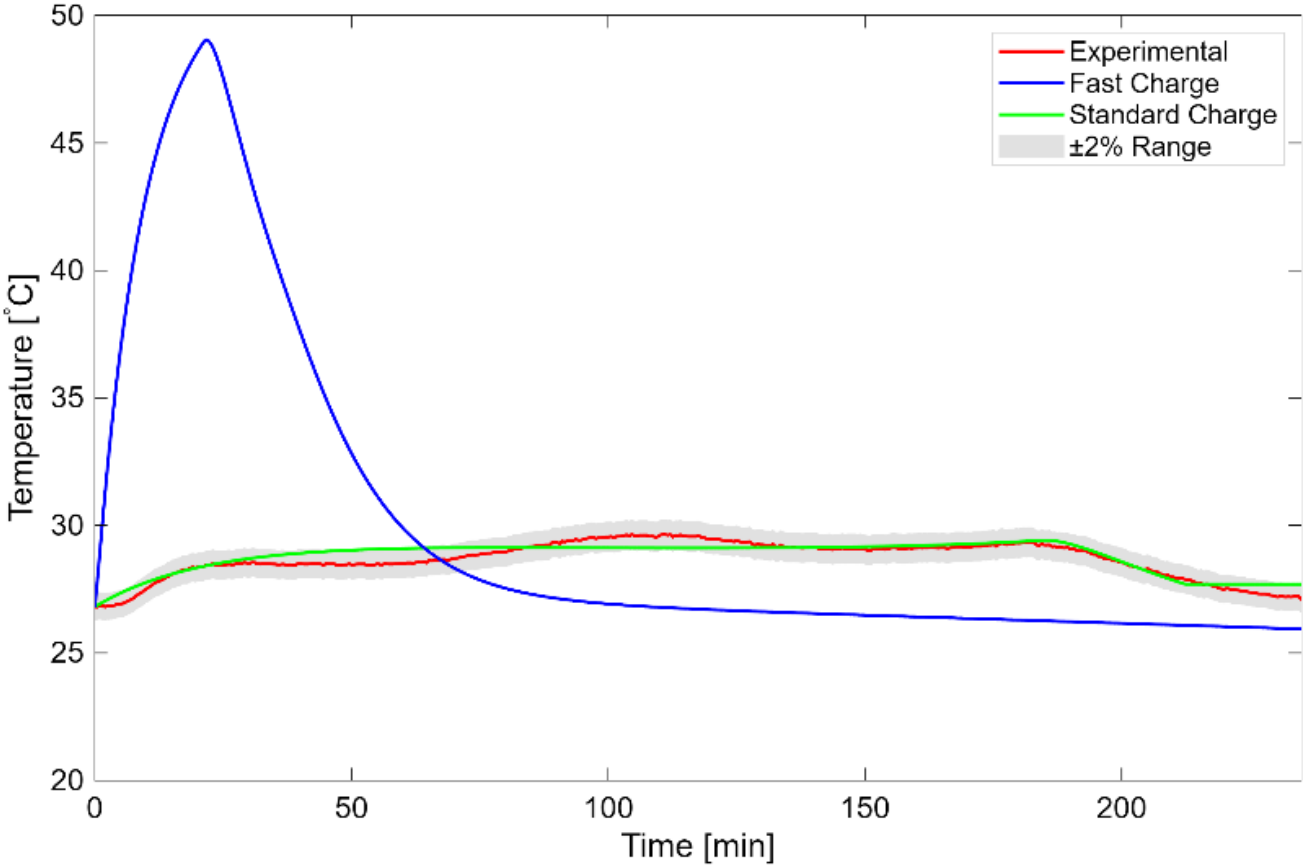

Figure 7. Validation of battery temperature model against experimental case study for standard and fast-charge cycles.

4.2 PCM case

To determine the optimal melting temperature of the PCM, the peak PCM temperature was found from sensible heat alone, at which point the latent component could be added, where a melting temperature of 28℃ was selected to sit just above the case ambient condition of 26℃, ensuring the latent heat storage is not triggered by ambient temperature alone, whilst also remaining within the optimal battery operating temperature range. A higher melting temperature would provide greater resistance to premature melting but would also increase the sensible heating requirement before latent storage is possible, overall reducing system thermal storage efficiency.

With the addition of the PCM, it is expected that the constant temperature during the melting phase will cause a reduction in the peak battery temperature, due to the high rate of heat absorption. This relationship is reflected in Figure 8, with an approximate 7.5% reduction in peak temperature, reducing from approximately 49.5 to 45.9℃ at the base case of PCM parameters and a thickness, $x_{pcm} = 44mm$.

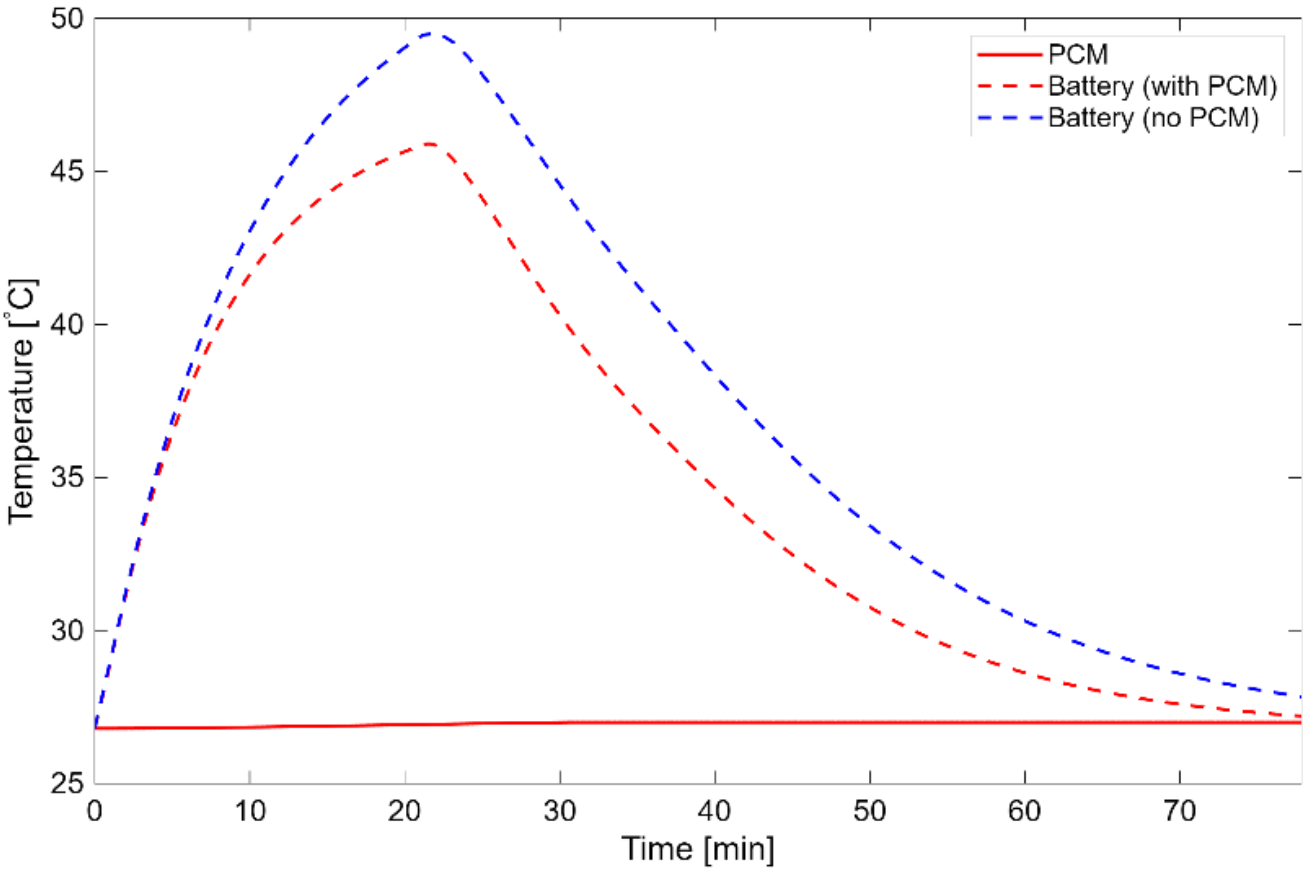

Figure 8. Battery Temperature profile with PCM addition.

Despite this result, however, the peak battery temperature still sits outside of the optimal range, as previously mentioned to have its upper limit at around 30℃, suggesting that the cooling capabilities of a passive PCM on its own are not enough to cool a fast-charging battery, or there is need for PCM parameter optimisation. This is mitigated by considering a sweep of PCM mass, and subsequently thickness due to a fixed contact area, values to ensure that the conduction resistance, due to the low thermal conductivity of paraffin-based PCMs, is not a limiting factor of the energy storage efficiency.

4.3 PCM sensitivity

Using the same simulation setup, a variety of mass and thickness values were considered, as well as the liquid volume fraction and were compared to their impact against the peak battery temperature. Figure 9 shows the results of the sensitivity analysis, which suggest that a lower mass and thickness results in a greater volume fraction and therefore more efficient thermal energy storage due to the reduction of unused PCM mass. A similar conclusion is also drawn from the peak battery temperature, which also decreases in a comparable manner, due to the decreased thermal resistance compared to the base case. The lowest case considered was a mass of 2kg, with a thickness of 4.4mm, providing a reduction of peak temperature to approximately 37.8℃ (21.7% reduction from no-PCM case; 14.2% reduction from base PCM parameters).

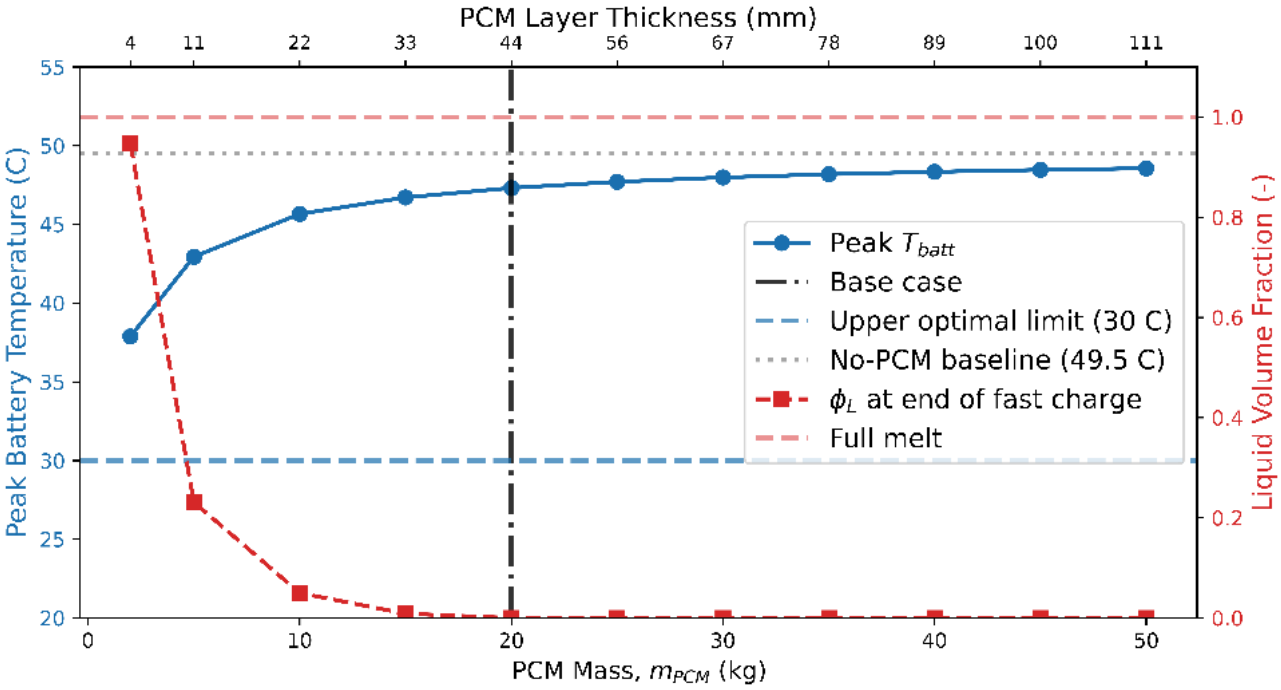

Figure 9. PCM Parameter sensitivity analysis.

However, the peak battery temperature remains above the upper optimal limit, which continues to suggest that the passive cooling capability of the PCM requires further support. This could be assisted by either a forced convection system, forcing heat through the battery and towards the PCM, or an investigation into the optimal PCM placement around the battery pack. Despite this, there is still a case to be made on the role of PCMs in helping to downsize other cooling components, as the amount of cooling required is still being reduced.

4.4 Thermal storage potential

Considering the final liquid volume fraction of the base case ($m_{pcm} = 20kg, x_{pcm} = 44mm$) shows that the PCM does not reach its melting point, meaning that $\phi_L = 0$ over the time of a fast-charge cycle and therefore no latent energy is stored, as the sensible heat component does not reach melting temperature. Further considering the lowest mass case, $m_{pcm} = 2kg$, a greater liquid volume fraction ($\phi_L = 0.948$) shows that the melting temperature is reached and sustained for long enough to store a significant amount of latent heat Q_{stored} (303kJ), calculated using eqn. (6). The total stored energy for each case is shown in Table 2.

$$Q_{stored}[kJ] = \phi_L m_{pcm} L \tag{6}$$

Table 2. Stored Latent Heat for each PCM case.

$m_{pcm}[kg]$	$\phi_L[-]$	$Q_{stored}[kJ]$	$Q_{stored}[Wh]$
2	0.948	303.36	84.3
5	0.231	184.8	51.3
10	0.050	80	22.2
15	0.009	21.6	6
20	0.000	0	0
25	0.000	0	0
30	0.000	0	0
35	0.000	0	0
40	0.000	0	0
45	0.000	0	0
50	0.000	0	0

The best considered case of approximately 300kJ (84.3Wh) stored is sufficient for the implementation of heat removal from the PCM to distribute the heat between the cabin and battery pack during driving. The positive impact of the LHTES can be quantified through the amount of heat required to raise battery pack temperature from a cold start condition using the standard sensible heat energy balance, $m_{bat}C_p\Delta T$. Considering a cold start at 0℃, the battery pack considered in this study would require approximately 222kJ (62Wh) of heat to enter the optimal temperature zone, leaving approximately 80kJ (22Wh) (28%) energy stored in the PCM to account for thermal losses during heat transport.

5 Conclusion

This work has investigated the role and viability of PCMs in a passive cooling and waste heat recovery capacity during fast-charging for an open-case battery module which would not allow a more commonly presented approach of embedding PCM in-between cells. A lumped thermal model was employed and simulated through MATLAB Simulink and validated against experimental data for a standard charge cycle, with results consistently within $\pm 2\%$ and a root mean square error of 0.35.

For the fast-charge case, the addition of the PCM reduced peak battery temperature by approximately 7.5% in the base configuration (20kg, 44mm thickness), from 49.5℃ to 45.9℃, and was further optimised through a sensitivity analysis, which revealed that a more compact configuration yields a higher liquid volume fraction and therefore more efficient latent heat storage. The 2kg case achieved a peak temperature reduction of 21.7% relative to the no-PCM case.

However, in all cases, the peak battery temperature remains above the upper optimal bound of 30℃, which presents a limitation of this study, however the concept of using a LHTES module external to the battery as a pre-conditioning energy source has been shown to reduce the load on other heat generating components and therefore reducing battery load.

Overall, this work demonstrates that despite the passive cooling limitation of using PCMs and their inability to satisfy the cooling demands of fast charging, their role in waste heat capture and redistribution in EVs presents a case for integration within an active, hybrid heating and cooling system.

5.1 Future work

This study could be extended further into an experimental analysis, as well as full optimisation of PCM mass through a detailed sensitivity analysis to fully optimise PCM selection and properties. Technological developments can also be applied to this system via the implementation of preconditioning algorithms to optimise the end of the fast charge cycle to complete just before the car is used, alongside a controlled method of heat transport for increased efficiency.

Acknowledgements

This work was supported by the University of Lincoln Engineering and Physical Sciences Research Council and ENACT DLA [Grant Reference: EP/Z535242/1]

Nomenclature

Heat generation & energy

Symbol	Meaning	Unit
$Q_{battery}$	Battery Heat Generation	W
Q_{joule}	Joule Heating Term	W
Q_{rev}	Reversible Entropic Heat	W
Q_{TES}	Maximum heat storage capacity of Latent Heat Thermal Energy Storage	J
Q_{in}	Total heat input	J
Q_{PCM}	Heat absorbed by PCM	J
Q_{stored}	Stored Latent Heat	J

Electrical & electrochemical

Symbol	Meaning	Unit
$I(t)$	Input current at each time step	A
U	Open-circuit Voltage	V
V	Terminal Voltage	V
$R(SOC,T)$	Internal cell resistance as a function of cell temperature and state of charge	Ω
$\frac{\partial U}{\partial T}$	Entropic Coefficient	VK^{-1}

Thermal

Symbol	Meaning	Unit
T	Internal cell temperature	K or ℃
T_{cool}	Coolant Temperature	℃
T_{amb}	Ambient Temperature	℃
T_{pcm}	Phase-Change Material Temperature	℃
T_m	Phase-Change Material melting Temperature	℃
h	Convective heat transfer coefficient	$Wm^{-2}K^{-1}$
A	Cell surface area	m^2
k_{pcm}	Thermal conductivity of Phase-change material	$Wm^{-1}K^{-1}$
x_{pcm}	Phase-change material thickness	mm

Material properties

Symbol	Meaning	Unit
m	Mass	kg
m_{cell}	Cell mass	kg
m_{pcm}	Phase-change material mass	kg
m_{bat}	Battery module mass	kg
C_p	Specific heat capacity	$Jkg^{-1}K^{-1}$
L	Specific latent heat of fusion	Jkg^{-1}

Configuration

Symbol	Meaning	Unit
N_s	Number of cells in series	-
N_p	Number of cells in parallel	-
Q_n	Nominal cell capacity	Ah

State variables

Symbol	Meaning	Unit
SOC	State of Charge	-
ϕ_L	Liquid Volume Fraction	-

References

[1] S. S. Madani, C. Ziebert, and M. Marzband, 'Thermal Characteristics and Safety Aspects of Lithium-Ion Batteries: An In-Depth Review', *Symmetry*, vol. 15, no. 10, p. 1925, Oct. 2023, doi: 10.3390/sym15101925.

[2] A. M. Ralls *et al.*, 'The Role of Lithium-Ion Batteries in the Growing Trend of Electric Vehicles', *Materials*, vol. 16, no. 17, p. 6063, Sep. 2023, doi: 10.3390/ma16176063.

[3] G. R. Molaeimanesh, S. M. Mousavi-Khoshdel, and A. B. Nemati, 'Experimental analysis of commercial LiFePO4 battery life span used in electric vehicle under extremely cold and hot thermal conditions', *J. Therm. Anal. Calorim.*, vol. 143, no. 4, pp. 3137–3146, Feb. 2021, doi: 10.1007/s10973-020-09272-z.

[4] A. Gharehghani *et al.*, 'Progress in battery thermal management systems technologies for electric vehicles', *Renew. Sustain. Energy Rev.*, vol. 202, p. 114654, Sep. 2024, doi: 10.1016/j.rser.2024.114654.

[5] N. Hamid *et al.*, 'Challenges in thermal management of lithium-ion batteries using phase change nanocomposite materials: A review', *J. Energy Storage*, vol. 100, p. 113731, Oct. 2024, doi: 10.1016/j.est.2024.113731.

[6] X. Fang, H. Tian, M. Wu, Y. Qiu, H. Li, and L. Wang, 'A real-time feedback and adaptive control strategy for battery thermal management system', *Energy*, vol. 333, p. 137148, Oct. 2025, doi: 10.1016/j.energy.2025.137148.

[7] A. Sevault, K. Banasiak, J. Bakken, and A. Hafner, *A novel PCM accumulator for refrigerated display cabinet: design and CFD simulations*. 2018.

[8] E. Mandev, M. A. Ceviz, F. Afshari, and B. Muratçobanoğlu, 'Evaluating PCM heat battery as a range-saving solution for electric vehicle cabin heating', *Sustain. Energy Technol. Assess.*, vol. 76, p. 104270, Apr. 2025, doi: 10.1016/j.seta.2025.104270.

[9] H. Kim, J. Hong, H. Choi, J. Oh, and H. Lee, 'Development of PCM-based shell-and-tube thermal energy storages for efficient EV thermal management', *Int. Commun. Heat Mass Transf.*, vol. 154, p. 107401, May 2024, doi: 10.1016/j.icheatmasstransfer.2024.107401.

[10] E. Bryce, 'Understanding Electric Vehicle Battery Charging: Inspired by Elon Musk's Analogy'. [Online]. Available: https://www.bryceenergyservices.com/2024/09/27/understanding-electric-vehicle-battery-charging/

[11] C.-H. Chen, F. Brosa Planella, K. O'Regan, D. Gastol, W. D. Widanage, and E. Kendrick, 'Development of Experimental Techniques for Parameterization of Multi-scale Lithium-ion Battery Models', *J. Electrochem. Soc.*, vol. 167, no. 8, p. 080534, Jan. 2020, doi: 10.1149/1945-7111/ab9050.

[12] P. H. Niknam and A. Sciacovelli, 'Hybrid PCM-steam thermal energy storage for industrial processes – Link between thermal phenomena and techno-economic performance through dynamic modelling', *Appl. Energy*, vol. 331, p. 120358, Feb. 2023, doi: 10.1016/j.apenergy.2022.120358.

[13] T.-F. Yang, W.-M. Yan, P.-Y. Lin, C.-Y. Lin, C.-C. Yang, and U. Sajjad, 'Thermal management of 21700 Li-ion battery packs: Experimental and numerical investigations', *Appl. Therm. Eng.*, vol. 236, p. 121518, Jan. 2024, doi: 10.1016/j.applthermaleng.2023.121518.